

Molecular Oxygen Insertion Polymerization into Crystals of Tetrakis(alkoxycarbonyl)quinodimethanes

Takahito Itoh,^{*,†} Shinji Nomura,[†] Masaki Ohtake,[†] Takefumi Yoshida,[†] Takahiro Uno,[†] Masataka Kubo,[†] Atsushi Kajiwara,[‡] Kazuki Sada,[§] and Mikiji Miyata[⊥]

Department of Chemistry for Materials, Faculty of Engineering, Mie University, 1515 Kamihama-cho, Tsu-shi, Mie 514-8507, Japan; Department of Materials Science, Nara University of Education, Takabatake-cho, Nara 630-8528, Japan; Department of Chemistry and Biochemistry, Graduate School of Engineering, Kyushu University, 6-10-1 Hakozaki, Higashi-ku, Fukuoka 812-8581, Japan; and Department of Material and Life Science, Graduate School of Engineering, Osaka University and Handai FRC, 2-1 Yamadaoka, Suita Osaka 565-0871, Japan

Received December 26, 2003; Revised Manuscript Received August 4, 2004

ABSTRACT: Solid-state alternating copolymerization took place by molecular oxygen insertion in the crystals of 7,7,8,8-tetrakis(ethoxycarbonyl)quinodimethane (**1a**) and 7,7-bis(ethoxycarbonyl)-8,8-bis(methoxycarbonyl)quinodimethane (**1b**) to form highly crystalline needlelike white solids for **1a** and amorphous ones for **1b**. The polymer structures were confirmed by ¹H NMR, ¹³C NMR, IR, elemental analysis, powder XRD, and TGA measurements. However, in vacuo polymerizations of **1a** and **1b** in the solid state with heating and photoirradiation did not take place. 7,7,8,8-Tetrakis(methoxycarbonyl)quinodimethane (**1c**) did not undergo solid-state alternating copolymerization with oxygen even in the presence of oxygen, but instead it homopolymerized to form highly crystalline homopolymer. The difference in the solid-state polymerization reactivity was discussed on the basis of molecular packing in the crystals obtained by X-ray crystallography. In addition, it was found by ESR measurement that the solid-state alternating copolymerizations with molecular oxygen proceed by means of a radical mechanism.

Introduction

Solid-state polymerization implies that polymerization proceeds starting from bulk monomer crystals, and it has been divided into two classes: topotactic and topochemical polymerizations.¹ The former is the polymerization that provides a polymer with a specific crystal structure formed under control of the crystal lattice of the monomer, and the latter is the polymerization that proceeds with no movement of the center of gravity of the monomer molecule and only slight rotation of the monomer molecule around the gravity; that is, the crystallographic position and symmetry of the monomer crystals are retained in the resulting polymer crystals. Therefore, topochemical polymerization is a promising method to obtain polymers with highly controlled structures. A limited number of monomers such as derivatives of diacetylene,¹ 2,5-distyrylpyrazine,² triene and triacetylene,³ muconic acid and sorbic acid,⁴ and 7,7,8,8-tetrakis(alkoxycarbonyl)quinodimethane⁵ have been reported to undergo topochemical polymerizations, and they are known to have strict requirements of the monomer arrangements in the crystals. However, it is still difficult to predict and control the polymerization properties of compounds in the crystals because arrangements of monomers play a significant role. Further investigation of the crystal structures of monomers related with solid-state polymerizations should enable us to control the reactivities of the monomers and provide us models for the reaction pathway of the polymerization reactions.

Molecular oxygen is well-known as an oxidizing agent in the organic reactions⁶ and as an inhibitor and a retarder of radical polymerizations in polymer chemistry, and it acts as a monomer and is incorporated in the polymer backbone.⁷ Peroxide polymers can be synthesized from solution polymerizations of vinyl monomers⁸ such as styrene, methyl methacrylate, vinyl-naphthalene, and α -methylstyrene and unsubstituted quinodimethane⁹ with molecular oxygen, and their physicochemical behavior such as autopyroizability,^{10,11} autocombustibility,¹² speciality fuels,¹⁰ coating molding applications,¹³ and initiators¹⁴ has been investigated. Recently, it was reported that dibenzofulvene¹⁵ and alkyl sorbate¹⁶ copolymerized with molecular oxygen in the solid state to form a random and/or an alternating copolymer. However, these reports did not reveal the crystal structures of the monomers that are suitable for copolymerization with molecular oxygen. More recently, we found that 7,7,8,8-tetrakis(ethoxycarbonyl)quinodimethane (**1a**) copolymerized with molecular oxygen in the solid state to give a highly crystalline alternating copolymer and reported it as a preliminary result.¹⁷

In this work, we investigated the polymerizations of **1a**, 7,7-bis(ethoxycarbonyl)-8,8-bis(methoxycarbonyl)quinodimethane (**1b**) prepared as a novel monomer, and 7,7,8,8-tetrakis(methoxycarbonyl)quinodimethane (**1c**) in the solid state under air and in the presence of oxygen, and the relationship of the solid-state polymerization reactivity with their crystal structures was discussed.

Experimental Section

Materials. Benzene was washed with in sequence with concentrated sulfuric acid, water, a 5% aqueous sodium hydroxide, and again water, dried over anhydrous calcium chloride, refluxed over metal sodium, and then distilled.

[†] Mie University.

[‡] Nara University of Education.

[§] Kyushu University.

[⊥] Osaka University and Handai FRC.

* To whom correspondence should be addressed: Ph +81-59-231-9410; Fax +81-59-231-9410; e-mail itoh@chem.mie-u.ac.jp.

Tetrahydrofuran (THF) was refluxed over lithium aluminum hydride for 12 h and distilled, and then the distillate was distilled again over benzophenone–sodium. 2,2'-Azobis(isobutyronitrile) (AIBN) was recrystallized from methanol. Pyridine was distilled over potassium hydroxide. Titanium tetrachloride was distilled over copper powder under reduced pressure. Diethyl malonate was distilled under reduced pressure under nitrogen. Carbon tetrachloride was used without further purification. 4-[Bis(methoxycarbonyl)methylene]cyclohexanone¹⁸ and 7,7,8,8-tetrakis(methoxycarbonyl)quinodimethane (**1c**)⁵ were prepared by the methods reported previously. Yellow prisms of **1c** were obtained by the recrystallization from a mixture solution of chloroform/hexane (1/3 v/v).

Monomer Synthesis. 1,4-Bis[di(ethoxycarbonyl)methylene]cyclohexane (2a). Titanium tetrachloride (16 mL, 146 mmol) in carbon tetrachloride (32 mL) was added dropwisely under nitrogen to dry stirred THF (220 mL) cooled in an ice bath. Into this yellow mixture were added 1,4-cyclohexanedi-one (2.30 g, 20.5 mmol) and diethyl malonate (8.02 g, 50.1 mmol). Pyridine (24 mL) in THF (26 mL) was added to the resulting brown suspension over 1 h, and the reaction mixture was stirred at room temperature for 3 days. Water (150 mL) and chloroform (100 mL) were added to the reaction mixture, the organic layer was separated, and then the aqueous layer was extracted with chloroform (4 × 100 mL). The combined organic fractions were successively washed with saturated aqueous sodium chloride (100 mL) and aqueous sodium bicarbonate (100 mL), dried over anhydrous magnesium sulfate, and filtered, and then the solvent of the filtrate was evaporated under reduced pressure. The crude product was purified by column chromatography (SiO₂, chloroform) followed by recrystallization from hexane to give **2a** as white needles (3.47 g, 43%); mp 59–60 °C. IR (KBr): ν_{CH} 2940, $\nu_{\text{C=O}}$ 1688, $\nu_{\text{C=C}}$ 1610, $\nu_{\text{C-O}}$ 1232, 1050 cm⁻¹. UV–vis (CH₃CN): 215 ($\epsilon = 1.75 \times 10^4$) nm. ¹H NMR (CDCl₃): δ 4.26 (q, $J = 7.26$ Hz, 8H, CH₂), 2.76 (s, 8H, CH₂), 1.29 (t, $J = 7.26$ Hz, 12H, CH₃). ¹³C NMR (CDCl₃): δ 165.2 (C=O), 157.7 (γ C), 123.5 (γ C), 61.1 (CH₂), 29.4 (CH₂), 14.1 (CH₃). Anal. Calcd for C₂₀H₂₈O₈: H, 7.12; C, 60.59; O, 32.29. Found: H, 7.03; C, 59.85; O, 33.12.

1-[Di(ethoxycarbonyl)methylene]-4-[di(methoxycarbonyl)methylene]cyclohexane (2b). **2b** was synthesized as white needles in 66% yield from 4-[bis(methoxycarbonyl)methylene]cyclohexanone and diethyl malonate by the same method as the procedure of synthesizing **2a**; mp 52–54 °C. IR (KBr): ν_{CH} 2944, $\nu_{\text{C=O}}$ 1690, $\nu_{\text{C=C}}$ 1606, $\nu_{\text{C-O}}$ 1221, 1018 cm⁻¹. ¹H NMR (CDCl₃): δ 4.26 (q, $J = 7.26$ Hz, 4H), 3.77 (s, 6H), 2.75 (s, 8H), 1.29 (t, $J = 6.93$ Hz, 6H). ¹³C NMR (CDCl₃): δ 165.5 (C=O), 165.1 (C=O), 158.5 (γ C), 157.4 (γ C), 123.6 (γ C), 122.8 (γ C), 61.0 (CH₂), 52.1 (CH₃), 29.5 (CH₂), 29.4 (CH₂), 14.0 (CH₃). Anal. Calcd for C₁₈H₂₄O₈: H, 6.52; C, 58.73; O, 34.75. Found: H, 6.05; C, 59.01; O, 34.94.

7,7,8,8-Tetrakis(ethoxycarbonyl)quinodimethane (1a). **2a** (678 mg, 1.71 mmol) was dissolved in benzene (50 mL), and this solution was added as one portion to activated manganese dioxide (5.42 g) and molecular sieves 4 Å (2.84 g) in benzene (350 mL) at reflux. After stirring for 15 min at reflux, activated manganese dioxide and molecular sieves were removed by filtration, and the solvent was evaporated under reduced pressure. The crude yellow solids were purified by column chromatography (SiO₂, chloroform) followed by recrystallization from hexane to give **1a** as yellow needles (225 mg, 34%); mp 72–73 °C. IR (KBr): ν_{CH} 2938, $\nu_{\text{C=O}}$ 1690, $\nu_{\text{C=C}}$ 1639, $\nu_{\text{C-O}}$ 1209, 1044 cm⁻¹. UV–vis (CH₃CN): 360 ($\epsilon = 5.75 \times 10^4$) nm. ¹H NMR (CDCl₃): δ 7.45 (s, 4H, CH), 4.32 (q, $J = 7.26$ Hz, 8H, CH₂), 1.33 (t, $J = 7.26$ Hz, 12H, CH₃). ¹³C NMR (CDCl₃): δ 164.7 (C=O), 138.8 (γ C), 130.0 (CH), 126.1 (γ C), 61.7 (CH₂), 14.0 (CH₃). Anal. Calcd for C₂₀H₂₄O₈: H, 6.16; C, 61.22; O, 32.62. Found: H, 6.15; C, 60.77; O, 33.08.

7,7-Bis(ethoxycarbonyl)-8,8-bis(methoxycarbonyl)-quinodimethane (1b). **1b** was synthesized as yellow needles in 28% yield by the same method as the procedure of synthesizing **1a**; mp 57–58 °C. IR (KBr): ν_{CH} 2950, $\nu_{\text{C=O}}$ 1689, $\nu_{\text{C=C}}$ 1551, $\nu_{\text{C-O}}$ 1199, 1042 cm⁻¹. UV–vis (CHCl₃): 366 ($\epsilon = 7.92 \times 10^4$) nm. ¹H NMR (CDCl₃): δ 7.45 (d, $J = 10.56$ Hz, 2H), 7.45 (d, $J = 10.56$ Hz, 2H), 4.32 (t, $J = 10.89$ Hz, 8H),

3.85 (s, 6H), 1.31 (t, $J = 10.89$ Hz, 6H). ¹³C NMR (CDCl₃): δ 165.1 (C=O), 164.6 (C=O), 139.4 (γ C), 138.7 (γ C), 130.2 (CH), 129.9 (CH), 126.5 (γ C), 125.2 (γ C), 61.8 (CH₂), 52.7 (CH₃), 14.1 (CH₃). Anal. Calcd for C₁₈H₂₀O₈: H, 5.53; C, 59.34; O, 35.13. Found: H, 5.51; C, 59.14; O, 35.35.

Polymerization Procedure. Solid-State Polymerization. A given amount of crystals (**1a**, **1b**, or **1c**) was put in a Pyrex ampule, which was sealed either without degassing (in air) or with degassing under reduced pressure (in vacuo) or purged with oxygen and with nitrogen. Thermal polymerizations were carried out by setting the ampule in an oil bath at 35, 50, and 60 °C for a given time of polymerization. An aliquot of the reaction product in the ampule was taken out and dissolved in chloroform-*d*, and ¹H NMR spectra were measured in order to determine the conversion. Conversions were calculated from peak area ratios of quinoid protons of the monomer to phenylene protons of the polymer: peaks at 7.45 ppm and at 7.54 ppm for **1a** and peaks at 7.42–7.47 ppm and at 7.50–7.57 ppm for **1b**. When the polymerization took place completely, all measurements of the reaction products were carried out without purification by the dissolution–precipitation method. When the polymerization took place incompletely, 1 mL of chloroform was added to dissolve the residual, and the resulting solution was poured into large amount of hexane to deposit the polymer, which was washed several times with excess hexane and dried under reduced pressure. Photopolymerizations were carried out at 32–34 °C under UV irradiation by using a high-pressure mercury lamp (Fuji Glass Work Type HB-400, 400 W) at a distance of 12 cm. After irradiation, an aliquot of the reaction product in the ampule was taken out and dissolved in chloroform-*d*, and ¹H NMR spectra were measured to determine the conversion. The following procedure was similar to that for the thermal polymerization. If the reaction products were insoluble in chloroform, the products were washed with chloroform and dried under reduced pressure and weighed.

Solution and Melt Polymerizations. Given amounts of crystals (**1a** or **1b**), AIBN as an initiator, and benzene as a solvent for **1a** were placed in a Pyrex ampule, degassed by the freeze–thaw method (repeated three times), and then sealed. The ampule was set in a bath at 60 °C for 50 h for **1a** and at 65 °C for 24 h for **1b** and then opened. The reaction mixtures were directly for **1a** and after adding 1 mL of chloroform for **1b** poured into an excess hexane to deposit the polymers, which were purified by three cycles of redissolution and reprecipitation. Chloroform and hexane were used as the solvent and precipitant, respectively. The product was dried under reduced pressure at room temperature until a constant weight was attained.

Thermal Decomposition. White needlelike solids (187.8 mg) obtained by thermal polymerization of **1a** in the solid state were placed in a Pyrex glass tube, which was set in a bath at 150 °C for 15 min. The solids decomposed to form transparent viscous oil, which was purified by column chromatography (SiO₂, chloroform) to obtain 34 mg (18% yield) of 1,4-bis(ethoxalyl)benzene as colorless oil: IR (neat): ν_{CH} 2938, $\nu_{\text{C=O}}$ 1701, 1658, $\nu_{\text{C=C}}$ 1575, 1441, 1348, $\nu_{\text{C-O}}$ 1182 cm⁻¹. ¹H NMR (CDCl₃): δ 8.17 (s, 4H, aromatic), 4.48 (q, $J = 7.3$ Hz, 4H, CH₂), 1.44 (t, $J = 7.3$ Hz, 6H, CH₃). ¹³C NMR (CDCl₃): δ 185.2 (C=O), 162.7 (C=O), 136.7 (Ar), 130.3 (Ar), 62.8 (CH₂), 14.1 (CH₃).

Decomposition of a thermal solid-state polymerization product from **1b** (200 mg) in chlorobenzene at 120 °C for 6 h produced 1-methoxyoxalyl-4-ethoxalylbenzene as colorless oil: ¹H NMR (CDCl₃): δ 8.17 (s, 4H, aromatic), 4.50 (q, $J = 6.93$ Hz, 2H, CH₂), 4.01 (s, 3H, CH₃), 1.44 (t, $J = 6.93$ Hz, 3H, CH₃).

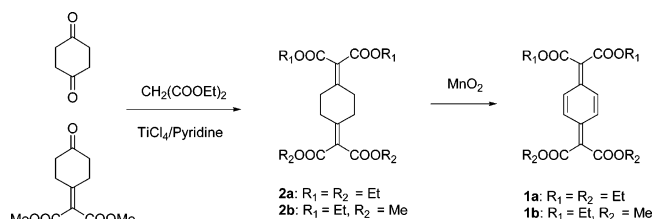
X-ray Crystallography. The powder X-ray diffraction (XRD) measurement of the products was carried out using Rigaku Rotaflex RU-200B in the 2 θ range from 5° to 60° at a scan speed of 0.5°/min with sampling width of 0.02°. The graphite-monochromated Cu K α radiation ($\lambda = 1.54178$ Å) was used with the power of the X-ray generator 40 kV and 150 mA. Single crystals were obtained by recrystallization from isopropyl ether for **1a**, hexane for **1b**, and a mixture of chloroform/hexane for **1c**. All single-crystal X-ray diffraction

Table 1. Thermal Polymerizations and Photopolymerizations of **1a**, **1b**, and **1c**

run no.	1a -c/mg	state	light source	atmosphere	temp/°C	time/h	convl/%	M_n^c
1a (Et)								
1	20.4	solid state	Hg lamp	air	34	25	15.7	1500
2	21.0		Hg lamp	vacuo	34	25	0	
3	11.1		dark	air	35	24	0	
4	10.5		dark	air	60	24	100	18000
5	10.1		dark	vacuo	60	24	0	
6	10.9		dark	N ₂	60	15	0	
7	11.4		dark	O ₂	60	15	100	18000
8 ^a	370	solution	dark	vacuo	60	50	72	2500
1b (Me, Et)								
9	100.4	solid state	Hg lamp	O ₂	32	48	22	1900
10	112.4		Hg lamp	vacuo	32	48	0	
11	100.7		dark	air	50	48	100	4100
12	100.7		dark	vacuo	50	48	0	
13	101.1		dark	N ₂	50	48	0	
14	100.4		dark	O ₂	50	48	100	3900
15 ^b	109.3	melt	dark	vacuo	65	24	58	51000
1c (Me)								
16	53.5	solid state	Hg lamp	O ₂	32	6	100	ND ^d
17	54.5		Hg lamp	vacuo	32	6	100	ND ^d
18	46.3		dark	O ₂	60	6	100	ND ^d
19	37.3		dark	vacuo	60	6	100	ND ^d

^a AIBN, 5.1 mg; solvent, benzene 1.0 mL. ^b AIBN, 4.9 mg. ^c Determined by GPC measurement using THF as an eluent and standard polystyrene as a reference. ^d Not determined (insoluble in common organic solvents).

Scheme 1



data were collected on a Rigaku RAXIS-RAPID imaging plate diffractometer using Cu K α radiation ($\lambda = 1.54178 \text{ \AA}$) monochromated with graphite. The structures were solved by the direct methods with the programs SIR88¹⁹ and SIR92²⁰ and refined by full-matrix least-squares procedures. All calculations were performed using the TEXSAN crystallographic software package of the Molecular Structure Corp.

Measurement. All melting points were obtained with a Yanaco MP-53 melting point apparatus. Elemental analyses were performed on a Yanaco CHN Corder MT-5 Instruments. The number-average molecular weights (M_n) of the polymers were estimated by gel permeation chromatography (GPC) on a JASCO PU-2080 Plus equipped with TOSOH UV-8020 ultraviolet (254 nm) detector and TSK gel G2500H₈ (bead size with 10 μm , molecular weight range 1.0×10^2 – 2.0×10^4) and TSK gel G3000H₈ (bead size with 10 μm , molecular weight range 1.0×10^2 – 6.0×10^4) using THF as an eluent at a flow rate of 1.0 mL/min and polystyrene standards for calibration. ¹H NMR and ¹³C NMR spectra were recorded on a JEOL JNM-EX 270 FT NMR spectrometer in chloroform-*d* with tetramethylsilane as an internal standard. Infrared spectra were obtained on KBr pellets with a JASCO IR-700 spectrometer. Thermogravimetric analysis (TGA) of the polymers was performed on a Seiko TG/DTA 220 Instruments at a scan speed of +5 °C/min under air. ESR measurement was performed on a JEOL JES RE-2X spectrometer operating in the X-band, utilizing a 100 kHz field modulation, and a microwave power of 1.0 mW. A TE₀₀₁ mode cavity was used. Temperature was controlled by a JEOL DVT2 variable-temperature accessory.

Results and Discussion

Monomer Synthesis. Monomers **1a** and **1b** were prepared by a synthetic route as shown in Scheme 1.

Knoevenagel condensations of 1,4-cyclohexanedione and 4-[bis(methoxycarbonyl)methylene]cyclohexanone

with diethyl malonate using titanium tetrachloride and pyridine as a dehydrating system²¹ gave 1,4-[bis(ethoxycarbonyl)methylene]cyclohexane (**2a**) in 43% yield and 1-[di(ethoxycarbonyl)methylene]-4-[di(methoxycarbonyl)methylene]cyclohexane (**2b**) in 66% yield, respectively, as white needles. Oxidations of **2a** and **2b** with activated manganese dioxide in refluxing benzene, followed by recrystallization from hexane, gave **1a** as yellow needles in 34% yield and **1b** as yellow needles in 25% yield, respectively.

Polymerization and Polymer Characterization. Crystals of **1a**, **1b**, and **1c** were polymerized under air or in vacuo by irradiation with a high-pressure Hg lamp at room temperature or by heating in the dark, and also solution polymerization of **1a** in benzene at 60 °C and melt polymerization of **1b** at 65 °C were performed for comparison. The results are summarized in Table 1.

When the crystals of **1a** were exposed to UV light at 34 °C in air or heated at 60 °C in air for 24 h, polymers formed as white needlelike solids in 15.6% and quantitative yields, respectively (runs 1 and 4). In contrast, **1a** did not polymerize in vacuo with irradiation or heating and under air in the dark or without heating (runs 2, 3, and 5). Therefore, polymer formation upon UV irradiation is due to photoinitiation, but not thermal initiation. These results strongly suggest the participation of oxygen in the polymerizations. To clarify role of oxygen in the polymerization, thermal polymerizations of **1a** in the solid state at 60 °C were performed in the presence of oxygen and nitrogen (runs 6 and 7). The monomer **1a** polymerized only in the presence of oxygen to give a polymer in a quantitative yield as white needlelike solids, but not in the absence of oxygen. This indicates that molecular oxygen truly participates in both thermal polymerizations and photopolymerizations in the solid state.

When crystals of **1b** were exposed to UV light at 32 °C in the presence of oxygen or heated at 50 °C in air for 48 h, polymers formed as white needlelike solids in 22.1% and a quantitative yields, respectively (runs 9 and 11). In contrast, **1b** did not polymerize in vacuo with irradiation and heating (runs 10 and 12). And also, the

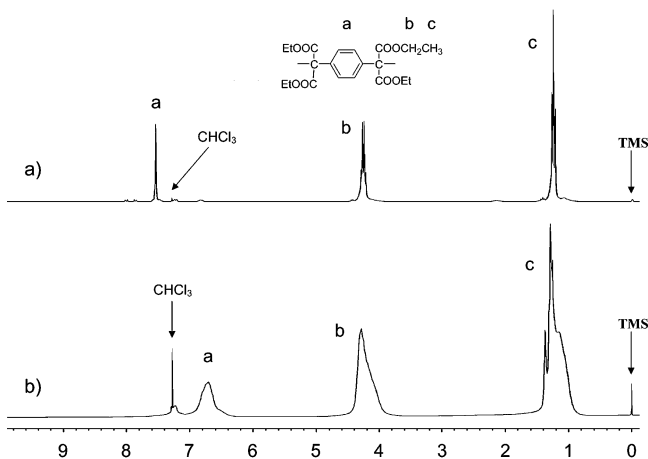


Figure 1. ¹H NMR spectra in chloroform-*d* of (a) an alternating copolymer of **1a** with oxygen (run 4) and (b) a homopolymer of **1a** (run 8).

participation of molecular oxygen in the polymerizations of **1b** in the solid state was confirmed by the polymerizations in the solid state in the presence of oxygen and nitrogen (runs 13 and 14). The polymerization behavior of **1b** was almost similar to that of **1a**. On the other hand, when crystals of **1c** were exposed to UV light at 32 °C or heated at 60 °C in the presence of oxygen and in vacuo for 6 h, all cases formed polymers as white crystalline solids, insoluble in common organic solvents, in almost quantitative yields (runs 16–19). The polymerization behavior of **1c** was significantly different from those of **1a** and **1b**.

White needlelike solids obtained by the thermal polymerizations of **1a** in the solid state at 60 °C (run 4) and of **1b** at 50 °C (run 11) were characterized by ¹H NMR and ¹³C NMR and IR spectroscopies, GPC, elemental analysis, and powder X-ray measurement. The data were also compared with those of the polymers obtained from the solution polymerization of **1a** (run 8) and from the melt polymerization of **1b** (run 15). On the other hand, the resulting polymer from **1c** was characterized only by IR spectroscopy and elemental analysis because of their insolubility in common organic solvents. Number-average molecular weights (*M_n*) were determined to be 18 000 for the polymer from the polymerization in the solid state and 2500 by the solution polymerization for **1a** and 4100 for the polymer from the polymerization in the solid state and 51 000 by the solution polymerization for **1b**. The ¹H NMR and ¹³C NMR spectra are shown in Figures 1 and 2 for the products obtained by the thermal solid-state polymerization in the presence of oxygen and the solution polymerization in the dark of **1a** and in Figures 3 and 4 for those obtained by the thermal solid-state polymerization in the presence of oxygen and the melt polymerization in the dark of **1b**, respectively, where each peak was assigned to the respective protons and carbons of chemical structures illustrated therein.

The polymers obtained by the solid-state polymerizations exhibited much sharper peaks than those obtained by the solution or melt polymerization. In the ¹H NMR spectrum of the polymer from **1a**, a peak at 7.53 ppm (a in Figure 1a) assigned to the phenylene protons of the polymer obtained by thermal solid-state polymerization was observed in a lower field compared to the corresponding one (6.6–6.9 ppm (a) in Figure 1b) of the polymer obtained by the solution polymerization. Also,

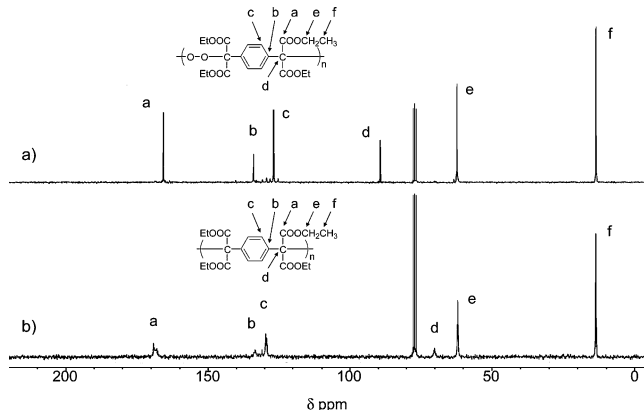


Figure 2. ¹³C NMR spectra in chloroform-*d* of (a) an alternating copolymer of **1a** with oxygen (run 4) and (b) a homopolymer of **1a** (run 8).

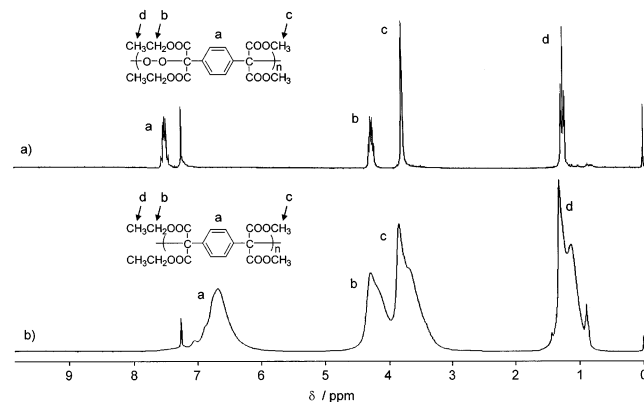


Figure 3. ¹H NMR spectra in chloroform-*d* of (a) an alternating copolymer of **1b** with oxygen (run 11) and (b) a homopolymer of **1b** (run 15).

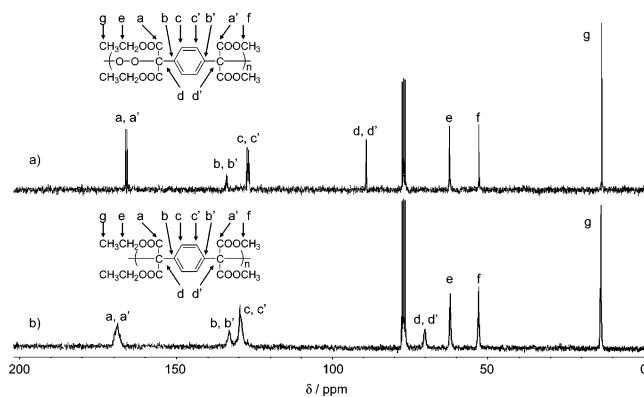


Figure 4. ¹³C NMR spectra in chloroform-*d* of (a) an alternating copolymer of **1b** with oxygen (run 11) and (b) a homopolymer of **1b** (run 15).

in the ¹³C NMR spectrum, the peak at 89.4 ppm (d in Figure 2a) assigned to the quaternary carbon atom in the solid-state polymerization polymer was observed 19 ppm further downfield than the corresponding one (70.0 ppm (d) in Figure 2b) in the solution polymerization polymer. For the polymer from **1b**, the chemical shifts assigned to the aromatic protons (7.52 ppm (a) in Figure 3a) in the ¹H NMR spectrum and the quaternary carbon (89.3 ppm (d, d') in Figure 4a) in the ¹³C NMR spectrum were observed in a lower field than the corresponding ones (6.3–7.0 ppm in Figure 3b and 70.0 ppm in Figure 4b) of the polymer obtained by the melt polymerization like as **1a**. These deshieldings observed

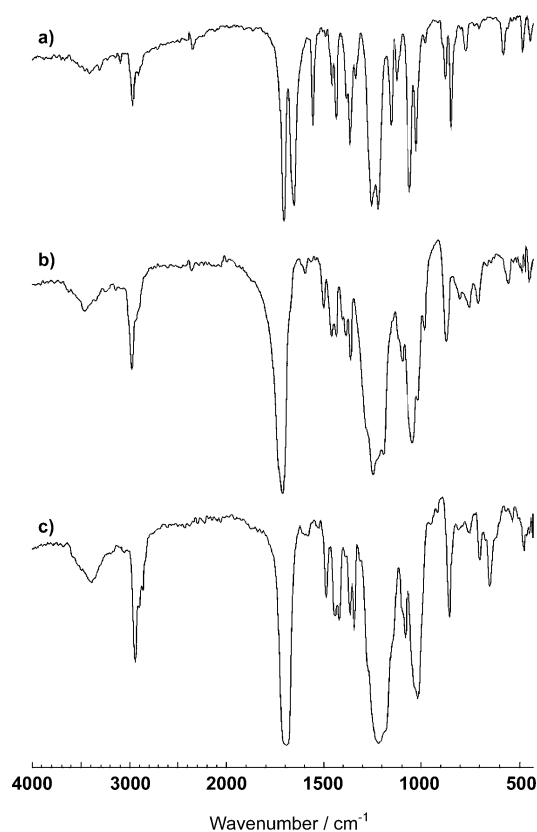


Figure 5. IR spectra (KBr) of (a) monomer **1a**, (b) an alternating copolymer of **1a** with oxygen (run 4), and (c) a homopolymer of **1a** (run 8).

in the NMR spectra indicate the presence of electron-withdrawing groups such as oxygen next to the units of **1a** and **1b** in the polymers.

The elemental analysis values (H, 5.62; C, 56.42; O, 37.96) of the polymer obtained from the solid-state polymerization of **1a** were in good agreement with the values (H, 5.70; C, 56.60; O, 37.70) calculated for an alternating copolymer of **1a** with molecular oxygen, but not with the found values (H, 6.10; C, 60.89; O, 33.01) for the homopolymer of **1a** obtained by the solution polymerization. The elemental analysis values (H, 5.08; C, 54.48; O, 40.44) of the polymer obtained from the solid-state polymerization of **1b** were in good agreement with calculated values (H, 5.09; C, 54.55; O, 40.36) as the 1:1 alternating copolymer of **1b** with molecular oxygen. In contrast, the elemental analysis values (H, 4.78; C, 56.93; O, 38.29) of the polymers obtained from the solid-state polymerization of **1c** in the presence of oxygen were in good agreement with the ones (H, 4.80; C, 57.14; O, 38.06) calculated for the homopolymer of **1c**.

IR spectra are shown in Figure 5 for the monomer and the polymer from the solid-state and solution polymerizations of **1a** and in Figure 6 for the monomer and the polymer from the solid-state and melt polymerizations of **1b**. A characteristic absorption band at 1550 cm^{-1} assigned to the exocyclic conjugated carbon-carbon double bond of **1a** and **1b** was absent in the IR spectra of the resulting products. The arising absorption bands at 1492 and 1411 cm^{-1} are assigned to carbon-carbon double bonds of the aromatic ring and that at 811 cm^{-1} is to out-of-plane deformation of the *para*-disubstituted benzene, which is characteristic for a two-

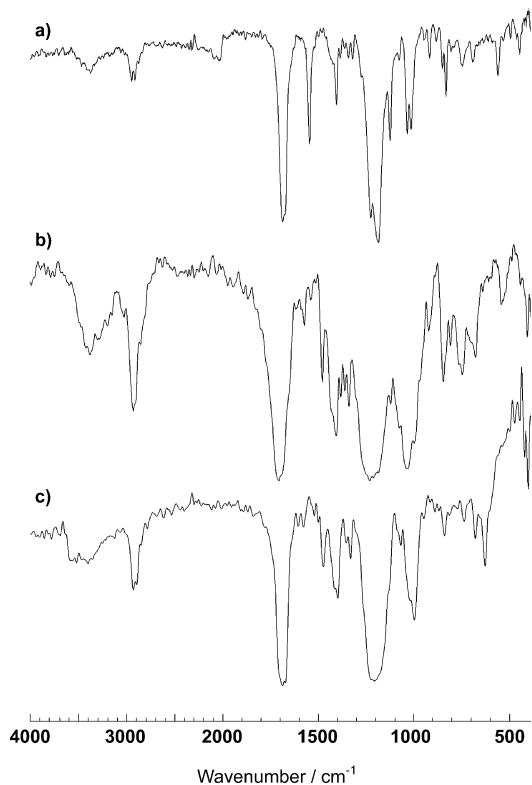


Figure 6. IR spectra (KBr) of (a) monomer **1b**, (b) an alternating copolymer of **1b** with oxygen (run 11), and (c) a homopolymer of **1b** (run 15).

adjacent-hydrogen system. These changes observed in the IR spectra support that this reaction follows the conventional mode observed for substituted quinodimethane molecules: the polymerization takes place at disubstituted exomethylene carbon atoms with formation of the corresponding stable aromatic structure.²² Unfortunately, a peak assigned to the peroxide group in the polymers obtained by the solid-state polymerization was not observed because of peak overlap with the C–O absorption assigned to the ester group. It is, therefore, concluded that the polymers obtained by the solid-state polymerization are the alternating copolymers of **1a** and **1b** with molecular oxygen. On the other hand, the IR spectrum of the polymer from **1c** obtained by the solid-state polymerization in the presence of oxygen was completely the same as the one obtained in vacuo and also identical to that of the homopolymer obtained from the solution polymerization of **1c** in benzene initiated by AIBN.⁵ These findings for **1c** indicate that the products from **1c** by the solid-state polymerizations in the presence of oxygen and in vacuo are the homopolymer of **1c**, and **1c** does not copolymerize with molecular oxygen.

The powder X-ray diffraction (XRD) patterns of monomers, polymers by solid-state polymerization, and the polymers reprecipitated from chloroform–hexane are shown in Figure 7. For the solid-state polymerization of **1a**, the relatively sharp diffraction patterns were observed at the reaction mixtures at conversions of 46% and 86% and even at 100% conversion. This indicates that the monomer **1a** maintains the crystallinity during and after completion of the polymerization. However, the powder XRD patterns illustrated that the polymer reprecipitated from chloroform–hexane has no significant peaks, which implies changes to the amorphous state (Figure 7f). On the other hand, for the polymeri-

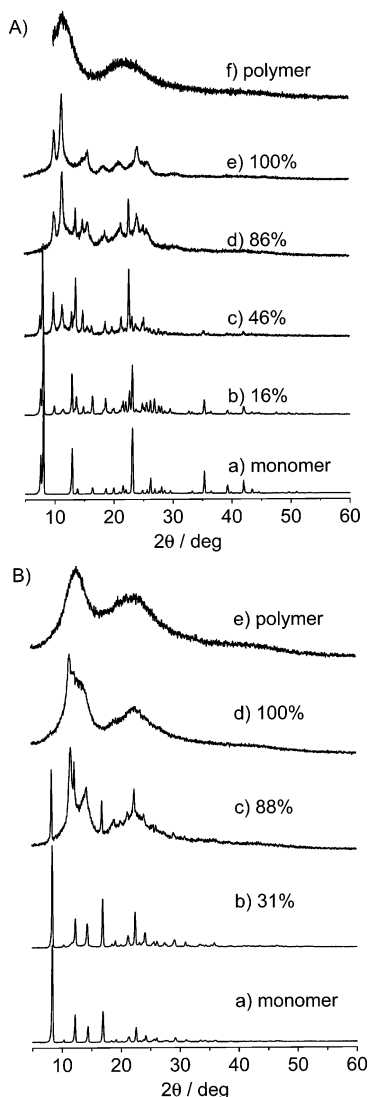


Figure 7. XRD patterns of (A) (a) monomer **1a**, (b) 16% conversion, (c) 46% conversion, (d) 86% conversion, (e) 100% conversion, and (f) reprecipitated polymer and (B) (a) monomer **1b**, (b) 31% conversion, (c) 88% conversion, (d) 100% conversion, and (e) reprecipitated polymer.

zation of **1b** in the solid state, the relatively sharp powder XRD patterns were observed until 88% but became broad at 100% conversion, indicating that the monomer **1b** has loss of the crystallinity during and after completion of the polymerization. Moreover, the powder XRD patterns illustrated that the polymer reprecipitated from chloroform–hexane has no significant peaks as well as the corresponding polymer from **1a**, and it is amorphous (Figure 7f). The changes observed in powder XRD patterns indicate that the thermal solid-state polymerizations of **1a** and **1b** proceed under the influence of the crystal lattice to form the alternating copolymer with a highly ordered crystal structure. The powder XRD patterns of the polymer from **1c** obtained by the solid-state polymerization in the presence of oxygen showed very sharp peaks even at complete conversion, and no loss of crystallinity was observed before and after the polymerization. This indicates that **1c** undergoes polymerization in topochemical mode even in the presence of oxygen to form highly crystalline homopolymer.

The thermal behavior of the polymers of **1a** and **1b** was investigated by TGA, and their TGA curves are

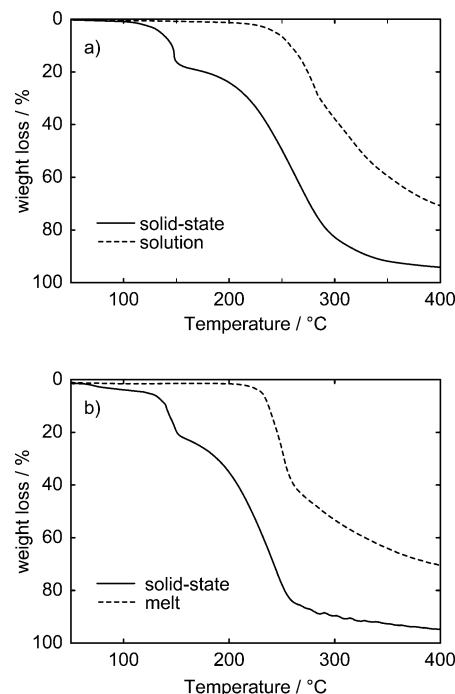
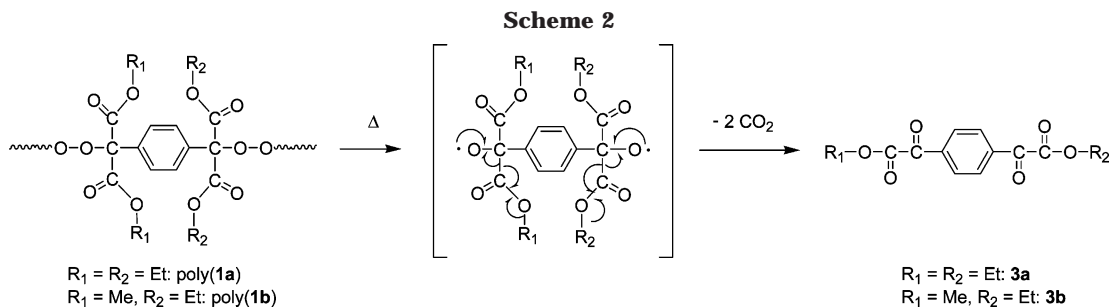


Figure 8. TGA curves of (a) (—) an alternating copolymer of **1a** with oxygen (run 4) and (---) a homopolymer of **1a** (run 8) and of (b) (—) an alternating copolymer of **1b** with oxygen (run 11) and (---) a homopolymer of **1b** (run 15).

shown in Figure 8. The TGA measurements showed that the solution polymerization polymer of **1a** and melt polymerization polymer of **1b** begin to decompose at about 210 °C, but the solid-state polymerizations show a two-stage decomposition and begin to decompose at about 110 °C for **1a** and at about 70 °C for **1b**. The weight losses from 110 to 150 °C for **1a** and from 70 to 150 °C for **1b** amount to 17% and 19%, respectively, which correspond approximately to the weight percent of an ethoxycarbonyl group from each unit of **1a** and **1b**. When the polymers from **1a** and **1b** obtained by the solid-state polymerization were heated at 150 °C for 15 min, 1,4-bis(ethoxalyl)benzene (**3a**) and 1-ethoxalyl-4-methoxalylbenzene (**3b**) were isolated in 18% and 15% yields, respectively, according to the mechanism as shown in Scheme 2. This indicates that both polymers have thermally degradable groups such as peroxide bonds.

The structure of active species from **1a** was directly investigated by ESR spectroscopy during thermal polymerization in the solid state under air. The ESR spectrum from crystals of **1a** under air at 62 °C in 30 min is shown in Figure 9a, where the ESR spectrum shows a broad triplet at a g value of 2.0030 with a coupling constant of 5.0 G. Coupling constants of the hydrogen at 2- and 6-positions of benzyl type radicals are reported to be about 5 G,²³ and also the observed ESR spectrum is in good agreement with the corresponding one simulated with the coupling constant of 5.0 G as shown in Figure 9b. Therefore, the observed ESR spectrum could be assigned to a propagating di-(ethoxycarbonyl)benzyl radical with the two equivalent hydrogens (Ha) at 2- and 6-positions of the phenylene group.

This result indicates that polymerization reaction of **1a** in the solid state takes place at the disubstituted exomethylene carbon atoms and proceeds through a



radical mechanism and that the propagating species is di(ethoxycarbonyl)benzyl radical. The radical concentration change during the polymerization reaction was investigated by ESR spectrometry using 2,2,6,6-tetramethyl-4-hydroxy-1-piperidinyloxy as a standard. Radical concentration increased rapidly with time and reached to a maximum value of 6.9×10^{-5} mol/kg in 1 h and then gradually decreased to 6.1×10^{-5} mol/kg in 2 h, 4.9×10^{-5} mol/kg in 3 h, 2.6×10^{-5} mol/kg in 21 h, and 2.3×10^{-5} mol/kg in 24 h. The decrease in the radical concentration after reaching to a maximum value is relatively small, and even after 100% conversion at 24 h, large amounts of radical are still alive. This indicates that a long-lived propagating radical is formed in this solid-state polymerization because of immobility of the polymer chain produced.

Crystal Structure and Packing of Molecules. To clarify the relationship of the molecular packing in the crystals with the polymerization reactivity, we investigated the crystal structures of **1a**, **1b**, and **1c** by X-ray crystallography. The crystallographic data of **1a**, **1b**, and **1c** are summarized in Table 2, and their crystal structures are shown in Figure 10. Unfortunately, in the crystal structure of **1b**, the terminal methyl groups of the ethoxycarbonyl groups are highly disordered, and the position of these methyl groups cannot be determined.

Table 2. Crystallographic Data for the Crystals of 1a, 1b, and 1c

parameter	1a	1b	1c
substituent	ethyl	ethyl; methyl	methyl
formula	C ₂₀ H ₂₄ O ₈	C ₁₈ H ₂₀ O ₈	C ₁₆ H ₁₆ O ₈
formula wt	392.40	364.35	336.29
crystal system	orthorhombic	monoclinic	monoclinic
space group	<i>Iba</i> 2	<i>P2</i> ₁ / <i>n</i>	<i>P2</i> ₁ / <i>n</i>
<i>a</i> , Å	13.483(2)	12.443(5)	8.6787(7)
<i>b</i> , Å	21.393(3)	5.108(1)	7.5719(7)
<i>c</i> , Å	6.8956(9)	14.466(5)	12.761(1)
α , deg	90	90	90
β , deg	90	101.76(1)	105.193(2)
γ , deg	90	90	90
<i>V</i> , Å ³	1988.9(5)	900.2(5)	809.2(1)
<i>Z</i>	4	2	2
ρ_{calc} , g/cm ³	1.310	1.344	1.380
unique reflcns	860	1638	1828
no. obsd reflns	832	1084	1477
<i>R</i> , <i>R</i> _w	0.291; 0.156	0.108; 0.200	0.106; 0.133
<i>R</i>	0.072	0.079	0.046
GOF	1.56	1.39	1.27
2 θ_{max} , deg	136.3	136.5	55.0
temp, °C	23	23	25

In the crystal structure of **1a**, the molecules form a one-dimensional column by the stacking of the quinodimethane rings along the crystallographic *c* axis. The stacking axes are nearly perpendicular to the molecular plane of the quinodimethane ring, and the stacked molecules are rotated successively by 60°. The face-to-face distance between units of **1a** in the stacked column is 3.4 Å, which corresponds to the π - π stacking distance of the aromatic rings.²⁴ The distance between the exomethylene carbon atoms in the column is 4.3 Å. This packing mode of the molecules of **1a** in the crystals is quite different from those found for **1c** as shown in Figure 10, which undergoes the homopolymerization. In the crystal structure of **1b**, the molecules construct another one-dimensional columnar structure by the stacking of the quinodimethane rings along the crystallographic *b* axis, and also the stacking axis is not perpendicular to the molecular plane of the quinodimethane rings like as **1c**. However, **1b** has a stacking distance ($d_s = 5.1$ Å) between the quinodimethane moieties and a distance ($d_{cc} = 5.1$ Å) between the exomethylene carbon atoms, which are greatly different from those ($d_s = 7.6$ Å and $d_{cc} = 3.9$ Å)⁵ of the topochemically polymerizable **1c**. Therefore, **1a** and **1b** do not undergo homopolymerization in the solid state, due to the inadequate molecular packing in the crystals.

Instead, both **1a** and **1b** copolymerized with molecular oxygen to form the alternating copolymers, and also they have maintained relatively high crystallinity until a conversion as high as about 80%. Molecular oxygen normally exists as a triplet (i.e., a diradical) in its ground state with a bond length of 1.2 Å, which is much shorter than the distance between the exomethylene carbon atoms for **1a** (4.29 Å) and for **1b** (5.1 Å). A

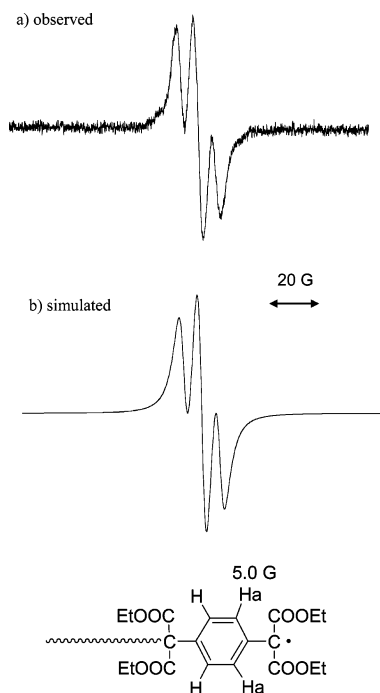


Figure 9. ESR spectrum of the propagating radical from **1a** crystals in 30 min under air at 62 °C: (a) observed and (b) simulated; Ha = 5.0 G.

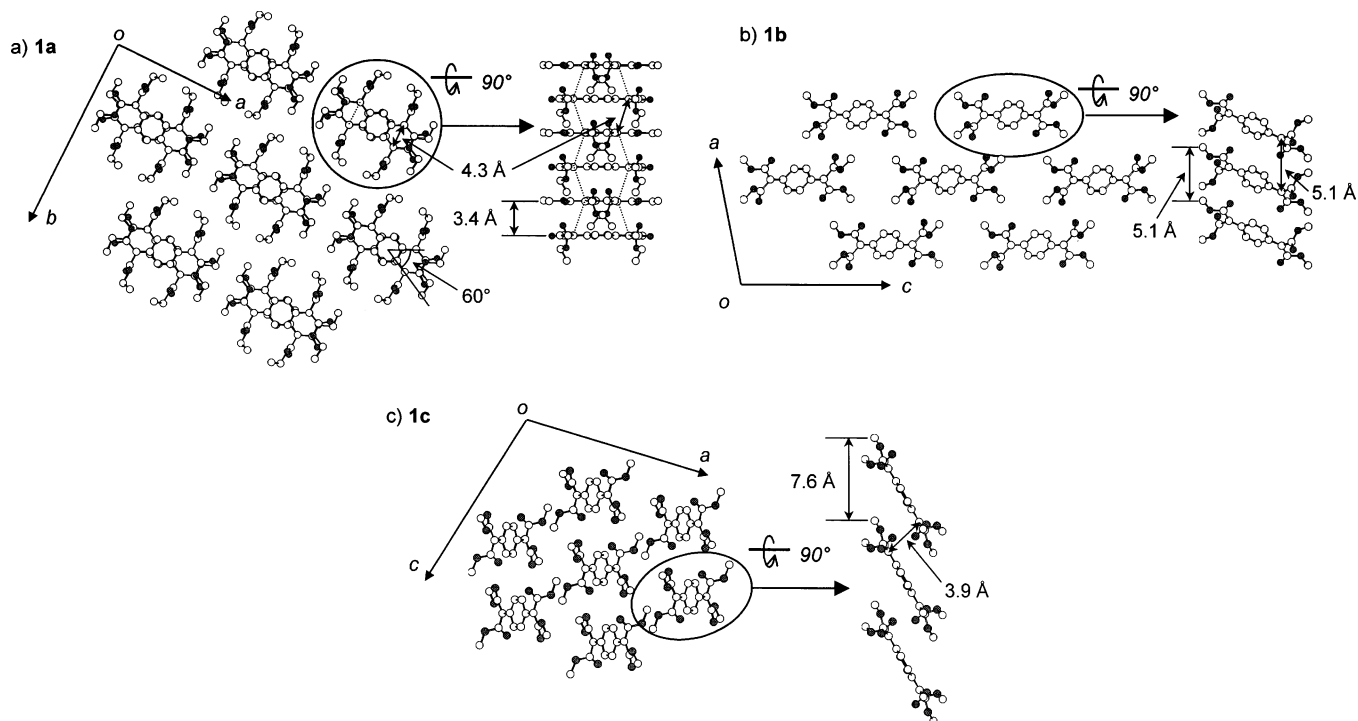


Figure 10. Crystal structures of (a) **1a**, (b) **1b**, and (c) **1c**. Open and solid circles represent carbon and oxygen atoms, respectively. Hydrogen atoms are omitted for clarity.

dioxygen unit may act as a hinge to bind neighboring quinodimethane molecules at their exomethylene carbon atoms. These distances are just suitable for the oxygen insertion into the polymer chains to yield the alternating copolymers. To clarify the polymerization mechanism, the molecular weights of the alternating copolymers produced at 60 °C in air were measured at different reaction times (3, 6, 9, 12, 18, and 24 h). They were in the range of 18 900 at the initial stage to 15 200 at the final stage with low molecular weight byproducts due to the slow decomposition of peroxide bond formed in the polymer, indicating that no significant changes in the molecular weight of the polymers was observed during the polymerization in the solid state. This suggests that the alternating copolymerization in the solid state proceeds by means of chain reaction mechanism. Tokitoh et al. reported that the reaction of overcrowded distibene with molecular oxygen in the solid state takes place through a single crystal to a single crystal process, and also a “domino” type reaction is caused by the oxidation of the molecules of distibene lying on the exterior surface of the single crystals.²⁵ Powder XRD measurements of **1a** and **1b** indicate that they retain relatively high crystallinity up to high conversion, and also **1a** maintains further the crystallinity up to much higher conversion than **1b**. It is, therefore, considered that the reactions of **1a** and **1b** with molecular oxygen start on the surface of their crystals and then proceed along a one-dimensional columnar of the crystals with the diffusion of molecular oxygen inside the crystals, though there are no decisive proofs to support fast diffusion of the molecular oxygen into the crystal lattice. The difference observed between **1a** and **1b** is considered to be attributed to (1) the shorter distance between the exomethylene carbon atoms in the **1a** crystals (4.3 Å) than in **1b** ones (5.1 Å), resulting in much slower collapse by smaller movement of the molecules of **1a** in the crystals, and (2) a smaller displacement between each column generated by the

polymerization of **1a** in comparison with **1b** because the crystals of **1a** have the hexagonal close packing structure and those of **1b** do not.

In summary, both **1a** and **1b** copolymerized spontaneously and alternately with molecular oxygen in the solid state to form highly crystalline needlelike white solids for **1a** and amorphous ones for **1b** by means of a radical mechanism, respectively. Alternating copolymer structures obtained by the thermal polymerization and photopolymerization in the solid state were confirmed by ¹H and ¹³C NMR, IR, elemental analysis, and TGA measurements. On the other hand, **1c** does not undergo solid-state alternating copolymerization with oxygen even under oxygen atmosphere, but instead it does the homopolymerization. No thermal and photopolymerizations of **1a** and **1b** in the solid state were observed in vacuo, which was explained by the lack of structural prerequisite for topochemical polymerization.

Acknowledgment. A part of this work was supported by “Nanotechnology Support Project” of the Ministry of Education, Culture, Sports, Science and Technology (MEXT), Japan.

Supporting Information Available: X-ray crystallographic files (CIF). This material is available free of charge via the Internet at <http://pubs.acs.org>.

References and Notes

- (1) (a) Wegner, G. *Z. Naturforsch. B* **1969**, *24*, 824. (b) Wenger, G. *Pure Appl. Chem.* **1977**, *49*, 443. (c) Enkelmann, V. *Adv. Polym. Sci.* **1984**, *63*, 91. (d) Ogawa, T. *Prog. Polym. Sci.* **1995**, *20*, 943. (e) Huntsman, W. D. *The Chemistry of Functional Groups. Supplement C: The Chemistry of Triple-Bonded Functional Groups*; Patai, S., Rappoport, Z., Eds.; John Wiley & Sons: New York, 1983; Chapter 22. (f) Okada, S.; Matsuda, H.; Nakanishi, H. *Polymeric Materials Encyclopedia*; Salamone, J. C., Ed.; CRC Press: Boca Raton, FL, 1996; p 8393. (g) Bloor, D.; Chance, R. R. *Polydiacetylenes*; NATO ASI Series E; Applied Sciences No. 102; Martinus Nijhoff: Dordrecht, 1985.

- (2) (a) Hasegawa, M. *Chem. Rev.* **1983**, *83*, 507. (b) Hasegawa, M. *Adv. Phys. Org. Chem.* **1995**, *30*, 117.
- (3) (a) Kiji, J.; Kaiser, J.; Wegner, J. G.; Schulz, R. C. *Polymer* **1973**, *14*, 433. (b) Enkelmann, V. *Chem. Mater.* **1994**, *6*, 1337. (c) Xiao, J.; Yang, M.; Lauher, J. W.; Fowler, F. W. *Angew. Chem., Int. Ed.* **2000**, *39*, 2132. (d) Hoang, T.; Lauher, J. W.; Fowler, F. W. *J. Am. Chem. Soc.* **2002**, *124*, 10656.
- (4) (a) Matsumoto, A.; Matsumura, T.; Aoki, S. *Macromolecules* **1996**, *29*, 423. (b) Matsumoto, A.; Yokoi, K.; Aoki, S.; Tashiro, K.; Kamae, T.; Kobayashi, M. *Macromolecules* **1998**, *31*, 2129. (c) Matsumoto, A.; Odani, T.; Chikada, M.; Sada, K.; Miyata, M. *J. Am. Chem. Soc.* **1999**, *121*, 11122. (d) Matsumoto, A.; Nagahama, S.; Odani, T. *J. Am. Chem. Soc.* **2000**, *122*, 9109. (e) Odani, T.; Matsumoto, A. *Macromol. Rapid Commun.* **2000**, *21*, 40. (f) Matsumoto, A.; Katayama, K.; Odani, T.; Oka, K.; Tashiro, K.; Saragai, S.; Nakamoto, S. *Macromolecules* **2000**, *33*, 7786. (g) Nagahama, S.; Matsumoto, A. *J. Am. Chem. Soc.* **2001**, *123*, 12176. (h) Matsumoto, A.; Odani, T. *Macromol. Rapid Commun.* **2001**, *22*, 1195. (i) Matsumoto, A.; Sada, K.; Tashiro, K.; Miyata, M.; Tsubouchi, T.; Tanaka, T.; Odani, T.; Nagahama, S.; Tanaka, T.; Inoue, K.; Saragai, S.; Nakamoto, S. *Angew. Chem., Int. Ed.* **2002**, *41*, 2502. (j) Matsumoto, A.; Tanaka, T.; Tsubouchi, T.; Tashiro, K.; Saragai, S.; Nakamoto, S. *J. Am. Chem. Soc.* **2002**, *124*, 8891. (k) Tanaka, T.; Matsumoto, A. *J. Am. Chem. Soc.* **2002**, *124*, 9676.
- (5) (a) Itoh, T.; Nomura, S.; Uno, T.; Kubo, M.; Sada, K.; Miyata, M. *Angew. Chem., Int. Ed.* **2002**, *41*, 4306. (b) Nomura, S.; Itoh, T.; Nakasho, H.; Uno, T.; Kubo, M.; Sada, K.; Inoue, K.; Miyata, M. *J. Am. Chem. Soc.* **2004**, *126*, 2035.
- (6) House, H. O. *Modern Synthetic Reactions*; W.A. Benjamin: New York, 1972; pp 337–352.
- (7) (a) Odian, G. *Principles of Polymerization*; John Wiley & Sons: New York, 1991; pp 259–266. (b) Bhanu, V. A.; Kishore, K. *Chem. Rev.* **1991**, *91*, 99.
- (8) (a) Cais, R. E.; Bovey, F. A. *Macromolecules* **1977**, *10*, 169. (b) Mukundan, T.; Kishore, K. *Macromolecules* **1987**, *20*, 2382. (c) Mukundan, T.; Kishore, K. *Macromolecules* **1989**, *22*, 4430. (d) Jayaseharan, J.; Kishore, K. *Macromolecules* **1997**, *30*, 3959.
- (9) Errede, L. A.; Hopwood, S. L., Jr. *J. Am. Chem. Soc.* **1957**, *20*, 6507.
- (10) Kishore, K.; Mukundan, T. *Nature (London)* **1986**, *324*, 130.
- (11) Nanda, A.; Kishore, K. *Indian J. Chem.* **2000**, *39A*, 1624.
- (12) Mukundan, T.; Annakutty, K. S.; Kishore, K. *Fuel* **1993**, *72*, 688.
- (13) Subramanian, K.; Kishore, K. *Eur. Polym. J.* **1997**, *33*, 1365.
- (14) (a) Nanda, A.; Kishore, K. *Polymer* **2001**, *42*, 2365. (b) Nanda, A.; Kishore, K. *J. Polym. Sci., Part A: Polym. Chem.* **2000**, *38*, 3665. (c) Nanda, A.; Kishore, K. *J. Polym. Sci., Part A: Polym. Chem.* **2001**, *39*, 546.
- (15) Nakano, T.; Nakagawa, O.; Yade, T.; Okamoto, Y. *Macromolecules* **2003**, *36*, 1433.
- (16) (a) Matsumoto, A.; Ishizu, Y.; Yokoi, K. *Macromol. Chem. Phys.* **1998**, *199*, 2511. (b) Matsumoto, A.; Higashi, H. *Macromolecules* **2000**, *33*, 1651. (c) Hatakenaka, H.; Takahashi, Y.; Matsumoto, A. *Polym. J.* **2003**, *35*, 640.
- (17) Nomura, S.; Itoh, T.; Ohtake, M.; Uno, T.; Kubo, M.; Kajiwara, A.; Sada, K.; Miyata, M. *Angew. Chem., Int. Ed.* **2003**, *42*, 5468.
- (18) Itoh, T.; Wanibe, T.; Iwatsuki, S. *J. Polym. Sci., Part A: Polym. Chem.* **1996**, *34*, 963.
- (19) Burla, M. C.; Camalli, M.; Cascarano, G.; Giacomazzo, C.; Polidori, G.; Spangna, R.; Viterbo, D. *J. Appl. Crystallogr.* **1989**, *22*, 389.
- (20) Altomare, A.; Burla, M. C.; Camalli, M.; Cascarano, G.; Giacomazzo, C.; Guagliardi, A.; Polidori, G. *J. Appl. Crystallogr.* **1994**, *27*, 435.
- (21) Lehnert, W. *Tetrahedron* **1973**, *29*, 635.
- (22) Itoh, T. *Prog. Polym. Sci.* **2001**, *26*, 1019.
- (23) (a) Krusic, P. J.; Kochi, J. K. *J. Am. Chem. Soc.* **1968**, *90*, 7155. (b) Neta, P.; Schuler, R. H. *J. Phys. Chem.* **1973**, *77*, 1368. (c) Hudson, A.; Hussain, H. A. *J. Chem. Soc. B* **1969**, 793.
- (24) (a) Dahl, T. *Acta Chem. Scand., Ser. A* **1988**, *42*, 1. (b) Williams, J. H.; Cockcroft, J. K.; Fitch, J. K. *Angew. Chem., Int. Ed. Engl.* **1992**, *31*, 1655. (c) Coates, G. W.; Dunn, A. R.; Henling, L. M.; Ziller, J. W.; Lobkovsky, E. B.; Grubbs, R. H. *J. Am. Chem. Soc.* **1998**, *120*, 3641.
- (25) Tokitoh, N.; Arai, Y.; Sasamori, T.; Okazaki, R.; Nagase, S.; Uekusa, H.; Ohashi, Y. *J. Am. Chem. Soc.* **1998**, *120*, 433.

MA035997F